

A Comparative Study of PDMS and PMMA Polymers Dielectric Touch Mode Capacitive Pressure Sensor

1
2
3
4
5
6

13
14
15

ABSTRACT

Aims: In this research work, a design method and a comparative of a touch mode capacitive pressure sensor (TMCPs) using poly-dimethyl-siloxane (PDMS) and poly-methyl methacrylate (PMMA) is the done. A novel method is proposed to linear the output characteristics of the sensor because planer type capacitive sensors are non-linear.

Study design: This method uses a mechanical coupler to convert the deflection of the diaphragm into a linear displacement that helps to linear the output characteristics. The mathematical model of the sensor is designed and simulated the 3D model to validate the mathematically calculated values.

Place and Duration of Study: This study is done in the Department of Electronics and Communication Engineering, Rajiv Gandhi University, Arunachal Pradesh at COMSOL Simulation Laboratory during 2021.

Methodology: The mechanical and electrostatic components of the sensor are represented mathematically model in two separate parts. For this study, a square diaphragm was used since it exhibits greater deflection than circular or rectangular diaphragms. In order to validate the model equation, a 3D model of a sensor is created in the COMSOL Multiphysics simulator and simulated. For the pressure range of 0.1 [MPa] to 10.1 [MPa], the identical 3D model of the sensor construction with a square diaphragm thickness of 20 μm is simulated for PDMS and PMMA. The different elements influencing the sensor's sensitivity are discovered, and the effects of the materials PDMS and PMMA on the output characteristic are discussed.

Results: The simulated and calculated sensitivity of the sensors based on PDMS are 0.03685 [fF/MPa] and 0.03467 [fF/MPa] respectively. And the simulated and calculated sensitivity of the sensors based on PMMA are 0.03929 [fF/MPa] and 0.03748 [fF/MPa] respectively. It is observed that the PDMS based TMCPs has more sensitivity then the PMMA based TMCPs.

Conclusion: The PMMA based TMCPs has higher sensitivity than the PDMS based TMCPs. The various parameters that affect the sensitivity of the sensor are diaphragm shape, size, Poisson's ratio and Young's modulus, area covered by the dielectric material, dielectric constant of the polymers dielectric and surface area of the electrode plate.

16
17
18

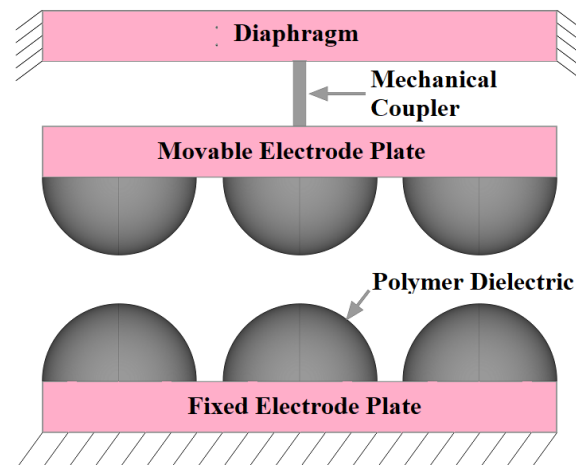
Keywords: Linear, Mechanical Coupler, Planer, Touch-mode, Sensitivity.

19 1. INTRODUCTION

20

21 There are various type of pressure sensors based on the physical sensing mechanisms,
 22 they are piezoelectric, piezoresistive, inductive, capacitive, untrasonics etc [1-5]. All these
 23 sensor also used in different application like turbulence flow sensing, mass colloidal flow
 24 sensing, wearables sensor, electronics skins [5-8][13]. There are three main varieties of
 25 capacitive pressure sensors. They are planar capacitive pressure sensors, comb structure
 26 capacitive pressure sensors, and touch mode capacitive pressure sensors [9-13]. In planar
 27 capacitive pressure sensor, the diaphragm structure does not come in contact with the
 28 bottom electrode plate, which is fixed. Such sensor is having lower sensitivity than the touch
 29 mode capacitive and they are nonlinear output with the input pressure. In touch mode
 30 capacitive pressure sensor, the diaphragm structure comes into contact with the dielectric
 31 which is attached to the bottom electrode plate. Such sensors provide a number of benefits,
 32 including a nearly linear output to input pressure relationship, a broad input range, and a
 33 robust design that can endure harsh environments. With the proper packing, this sensor can
 34 be used to measure fluid flow, acceleration, and force. In comb structure capacitive pressure
 35 sensor, this sensor structure has interdigitated fingers that resemble two combs interlocking.
 36 This construction had a larger surface area than the planar and touches mode structure,
 37 which enhanced the sensor capacitance. The comb structure capacitive pressure sensor has
 38 two modes of operation, transverse and longitudinal. This kind of sensor has high sensitivity
 39 by nonlinear output characteristic.

40 The output of a simple touch mode capacitive pressure sensor is nonlinear because the
 41 diaphragm deformed parabolically their structure while applying the pressure [8][11],
 42 therefore a modified touch mode capacitive pressure sensor with a mechanical coupler is
 43 proposed as shown in fig. 1. The mechanical coupler will transform the nonlinear
 44 deformation of the diaphragm plate into a linear displacement which will produce linear
 45 output characteristic.



46

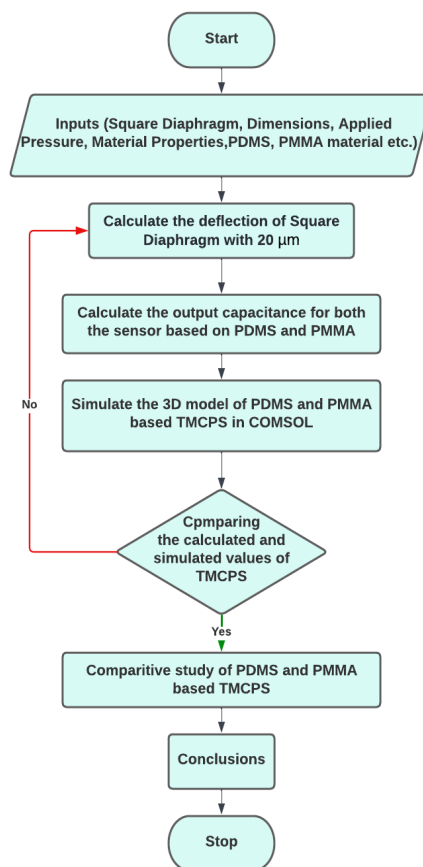
47 **Fig. 1: Modified structure of TMCP.**

48 The proposed structure has a diaphragm, mechanical coupler, movable plate, polymer
 49 dielectric and fixed plate. In the diaphragm, the pressure is applied and deflects. This
 50 deflection is converted in linear displacement by mechanical coupler which is attached
 51 between the diaphragm and movable plate. The movable plate moves toward the fixed plate
 52 which is separated by polymer. This polymer dielectric keeps the moveable plate away from
 53 touching the fixed plate.

54 2. MATERIAL AND DESIGN METHODOLOGY

55

56 The suggested approach measures the deflection of square diaphragms over a pressure
 57 range of 0.1 [MPa] to 10.1 [MPa] with step size 1 [MPa] in order to calculate the output
 58 capacitance of the modified TMCPS. The 3D modelsof TMCPS are proposed with the
 59 following specifications: the hemispheres ofPDMS and PMMA dielectric polymers with a
 60 radius of 40 [μm], the square diaphragm with a length of 300 [μm] and a thickness of 20
 61 [μm], and the square capacitor plates with a length of 300 [μm] and a thickness of 20 [μm].
 62 The deflection of the square diaphragm is calculated for the applied pressure then the output
 63 capacitances of the TMCPS based on PDMS and PMMA based TMCPS is calculated. The
 64 proposed 3D model is simulated with two different types of polymer dielectrics i.e., PDMS
 65 and PMMA. The verification of simulated and calculated values is done twice, one with the
 66 PDMS based sensor and another is with the PMMA based sensor.



67

68 **Fig. 2: The proposed methodology of design flow.**

69 A comparative study is carried out between the two sensors, one with the PDMS based
 70 sensor and another with the PMMA based sensor. After conducting a comparison analysis, a
 71 number of significant findings were drawn from the various observations. The proposed
 72 methodology of design flow is shown in fig. 2.

73 The touch mode capacitive pressure sensor is similar to other Micro-Electro-Mechanical
 74 systems. This typically consists of two parts: the mechanical and electrostatic parts. Hence,

75 mechanical and electrostatic components are mathematically calculated in accordance with
 76 their respective operating principles.
 77 In mechanical model, the diaphragm converts the applied pressure into the deflection. This
 78 deflection is converted into linear displacement by the mechanical coupler. For calculating
 79 the deflection of the square diaphragm, let us consider a rectangular diaphragm with a
 80 length of $2b$ which is in y -direction and breadth of $2a$ which is in x -axis. The total energy Ω
 81 of the rectangular diaphragm for applied pressure P is given as follow [14-16].
 82

$$83 \quad \Omega = \frac{D}{2} \int_{-b}^b \int_{-a}^a \left\{ \left(\frac{\partial^2 \psi(x,y)}{\partial x^2} + \frac{\partial^2 \psi(x,y)}{\partial y^2} \right)^2 - (1-\nu) \left[\frac{\partial^2 \psi(x,y)}{\partial x^2} \frac{\partial^2 \psi(x,y)}{\partial y^2} - \left(\frac{\partial^2 \psi(x,y)}{\partial x \partial y} \right)^2 \right] \right\} dx dy - \int_{-b}^b \int_{-a}^a \psi(x,y) P dx dy, \quad (1)$$

84 Where, $\Psi(x,y)$ = deflection function, D = flexural rigidity and ν = Poisson's Ratio. The value of
 85 D is given by

$$86 \quad D = \frac{Eh^3}{12(1-\nu^2)} \quad (2)$$

87 Where, h = thickness of the diaphragm and E = Young's Modulus. The deflection function
 88 $\Psi(x,y)$ of a rectangular diaphragm is given by [15-16]

$$89 \quad \psi(x,y) = \omega(a^2 - x^2)^2 (b^2 - y^2)^2, \quad (3)$$

90 Where ω = constant. From Eq.1 and Eq. 3 and applying the condition $\frac{\partial \Omega}{\partial \omega} = 0$, we get

$$91 \quad \omega = \frac{49P}{128(7a^4 + 4a^2b^2 + 7b^4)D} \quad (4)$$

92 Putting the value of ω into Eq. 3, The Eq. 3 becomes

$$93 \quad \psi(x,y) = \frac{49P}{128D(7a^4 + 4a^2b^2 + 7b^4)} (a^2 - x^2)^2 (b^2 - y^2)^2 \quad (5)$$

94 The side length of the square diaphragm is equal i.e., $a=b$, then Eq. 5 becomes

$$95 \quad \psi(x,y) = 0.02126 \frac{Pa^4}{D} \left(1 - \frac{x^2}{a^2}\right)^2 \left(1 - \frac{y^2}{a^2}\right)^2. \quad (6)$$

96 Eq. 6 is the deflection function at (x,y) point of a square diaphragm. At the centre of the
 97 diaphragm i.e. $(x,y)=(0,0)$, the maximum deflection of a square diaphragm is occurred and is
 98 given by

$$99 \quad \psi(x,y)_{\max} = \psi(0,0) = \psi = 0.02126 \frac{Pa^4}{D}$$

$$100 \quad \psi(x,y)_{\max} = \psi(0,0) = \psi = 0.25512 \frac{Pa^4}{Eh^3} (1-\nu^2) \quad (7)$$

101 From Eq. 7, the maximum deflection of the diaphragm is depending on the Poisson's ratio,
 102 Young's modulus, thickness of the diaphragm, length of the square diaphragm, and applied
 103 pressures.

104 In electrostatic modeling, fig. 1 displays a design model for the TMCPS using PDMS or
 105 PMMA as the polymer dielectric material. Hemispherical polymers are used to coat portions
 106 of the electrode plates, but not all of them. The surfaces of the electrodes are separated into
 107 two sections: one section is the portion of the electrodes covered in dielectric polymers, and
 108 the other section is the remainder of the electrode surface that is uncoated.

109 As a result, the sum of capacitances C_1 and C_2 can be used to compute the overall
 110 capacitance C . Where C_1 denotes the capacitance of the dielectric polymer-covered area
 111 and C_2 denotes the capacitance of the uncovered area.

112 $C = C_1 + C_2,$ (8)

113 Now, the value of C_1 and C_2 can be calculated by

114 $C_1 = n \frac{\epsilon_0 \epsilon_r}{(g - \psi)} \pi r^2,$ (9)

115 $C_2 = \frac{\epsilon_0 (\alpha - n\pi r^2)}{(g - \psi)},$ (10)

116 Where, r = radius of the hemisphere, n = number of hemispherical polymer dielectric, ϵ_0 =
 117 absolute permittivity, ϵ_r = relative permittivity, α = surface area covered of the electrode plate
 118 and g = gap between the electrodes. Now, the total capacitance of the TMCPS is

119 $C = \frac{\epsilon_0 (\alpha + n\pi r^2 (\epsilon_r - 1))}{(g - \psi)},$ (11)

120 The sensitivity of the sensor S is ratio of change in the output to the change in input.
 121 Mathematically the sensitivity can be express for TMCPS is

122 $S = \frac{\epsilon_0 (\alpha + (\epsilon_r - 1)n\pi r^2)}{P(g - \psi)}.$ (12)

123 From Eq. 12, the sensitivity of the sensor is depending on the total area covered by the of
 124 the polymer dielectric hemisphere, surface area of the electrode, gap between electrodes,
 125 relative permittivity and all the parameters that affect the deflection i.e., Poisson's ratio,
 126 Young's modulus of the diaphragm's materials, thickness of the diaphragm, length of the
 127 square diaphragm, and applied pressures.

128 Tables should be explanatory enough to be understandable without any text reference.
 129 Double spacing should be maintained throughout the table, including table headings and
 130 footnotes. Table headings should be placed above the table. Footnotes should be placed
 131 below the table with superscript lowercase letters.

132

133 **3. RESULTS AND DISCUSSION OF SIMULATED 3D MODEL OF TMCPS**

134 The COMSOL Multiphysics simulator was used to simulate the 3D model of the TMCPS
 135 based on PDMS and PMMA, which is depicted in fig. 1. This model contains a square
 136 diaphragm, mechanical coupler, moving electrode plate, fixed electrode plate, and a
 137 numbers of hemisphere-shaped dielectric polymers. The mechanical coupler is used to
 138 transform the deflection into linear displacement. Table 1 tabulates the physical dimension of
 139 the various TMCPS components, while table 2 tabulates the material properties of TMCPS
 140 components.

141 **Table 1: Physical dimension of the TMCPS's components.**

TMCPS Components	Material	Dimensions		
		Length	Breath	Thickness/ Radius
Diaphragm	Gold	300 [μm]	300 [μm]	20 [μm]
Mechanical Coupler	Silicon-dioxide	20 [μm]	20 [μm]	20 [μm]
Electrode Plates	Gold	300 [μm]	300 [μm]	20 [μm]
Polymer Dielectric	PMMA/PDMS	-	-	40 [μm]

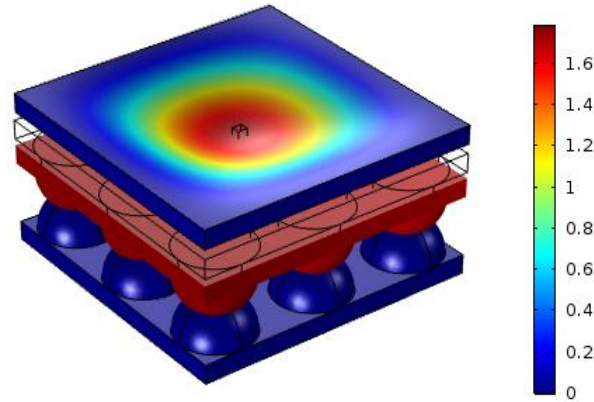
142

143 **Table 2: Material properties of the TMCPS components.**

Material	Young's modulus	Poisson's ratio	Dielectric Constant
Gold	70 [GPa]	0.425	-
Silicon dioxide	70 [GPa]	0.17	-
PDMS	-	-	2.4
PMMA	-	-	3

144

145 After designing the 3D model of the TMCPS in the COMSOL simulator, the material
 146 properties of the various components are defined in the simulator. The mechanical and
 147 electrostatic are configured and the applied pressure is also defined in the global variable. A
 148 parametric swap is done in COMSOL for input pressure starting from 0.1 [MPa] to 10.1
 149 [MPa] with a step size of 1 [MPa].



150

151 **Fig. 3: COMSOL simulation output showing the deflection and shifting of movable**
 152 **electrode plate.**

153 In table 3, the deflection values that were calculated and simulated for both PDMS and
 154 PMMA based TMCPS are listed. The deflection is same for all both the sensors as the
 155 diaphragm is of same material for both the sensor. Also, it has been found that as increases
 156 in applied pressure, the deflection increases also increase.

157 **Table 3: Calculated and simulated values of deflections.**

Pressure [MPa]	Sim [μm]	Cal [μm]
0.1	0.01742	0.0186
1.1	0.19167	0.2046
2.1	0.3658	0.3906
3.1	0.5398	0.5766
4.1	0.7136	0.7625
5.1	0.8872	0.9485
6.1	1.0611	1.1345
7.1	1.2339	1.3205
8.1	1.4076	1.5065
9.1	1.5791	1.6924
10.1	1.7516	1.8784

158

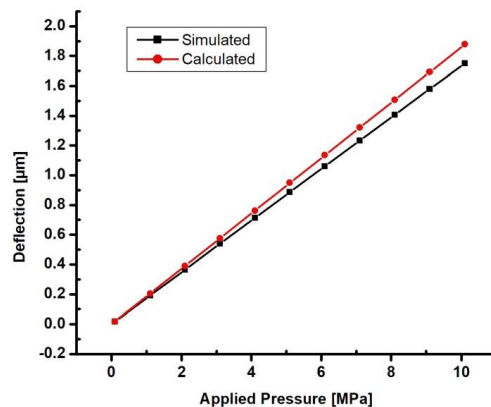
159 The simulated and calculated capacitance values for the proposed TMCPS are shown in
 160 table 4. The output capacitance is in the fF range, as can be observed from the data. The
 161 values also increase as the applied pressure is increased. The PMMA sensor has higher
 162 capacitance values than the PDMS sensor, the reason is PMMA has higher dielectric values
 163 than PDMS.

164 **Table 4: Calculated and simulated values of capacitance.**

Pressure [MPa]	PDMS-TMCPS [fF]		PMMA-TMCPS [fF]	
	Sim	Cal	Sim	Cal
0.1	16.7187	16.4263	17.1025	17.7623
1.1	16.7546	16.4603	17.1408	17.7991
2.1	16.7908	16.4945	17.1793	17.8360
3.1	16.8272	16.5288	17.2181	17.8731
4.1	16.8638	16.5632	17.2571	17.9103
5.1	16.9006	16.5978	17.2963	17.9477
6.1	16.9376	16.6326	17.3357	17.9853
7.1	16.9747	16.6674	17.3753	18.0230
8.1	17.0120	16.7025	17.4152	18.0609
9.1	17.0496	16.7377	17.4552	18.0989
10.1	17.0872	16.7730	17.4954	18.1371

165

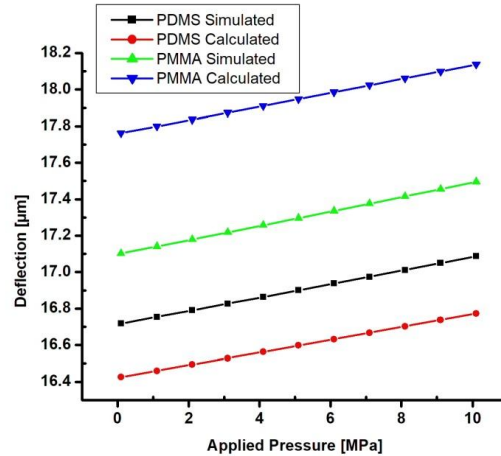
166 The graphic representations of table 3 are shown in fig. 4. The simulated and calculated
 167 deflections are seen to linearly change with the applied pressures..



168

169 **Fig. 4: Calculated and simulated deflections values for the applied pressures.**

170 Additionally, it has been noted that although the calculated values and simulated values are
 171 practically identical and the calculated values are slightly higher than the simulated values.
 172 So the mathematical model of the deflection can be used for further study. This linearly
 173 deflection at the center of the diaphragm is translated to linear displacement by the
 174 mechanical coupler. Because of this linear translation the output capacitance of the sensor is
 175 linear in characteristics.



176
177
178

Fig. 5: Calculated and simulated output capacitance values for the applied pressures.

179 Fig. 5 illustrates is the graphical representation of table 4. The simulated and calculated
180 values of output capacitance are also linear with those of input pressure. The simulated
181 output values are less than the calculated values but they are much closed. The PDMS
182 based sensor has less sensitive then the PMMA based sensor. This is because the dielectric
183 coefficient of the PDMS is lower than the dielectric coefficient of the PMMS. As the output
184 values are much closed we can used the proposed mathematical model of the sensor in
185 future application. The proposed improved model of the touch mode capacitive pressure
186 sensor is very linear compared to the nonlinear planar touch mode capacitance pressure
187 sensors. From the mathematical model, the various factor affecting the sensitivity of the
188 sensor can be found.

189
190
191

4. CONCLUSION

192 This research study focuses on the mathematical modeling and simulation of the touch
193 mode capacitive pressure sensor for pressure ranges of 0.1 [MPa] to 10.1 [MPa]. A design
194 method based on PMMA and PDMS is presented and realized for a touch mode capacitive
195 pressure sensor. Due to the strong agreement between the simulated and calculated values,
196 the mathematical expression can be used to find the various factors impacting on the
197 sensitivity of the sensors. The deflection if the diaphragm is increases with the applied
198 pressure and surface area of the diaphragm. The deflection of the diaphragm is decrease
199 with increase in Young's modulus, thickness of the diaphragm and Poisson's ratio as it has
200 negative values. The output capacitances are increase with increase in deflection, area
201 covered by the dielectric materials and relative permittivity of the dielectric but decrease
202 with increase in the gaps between the two electrode plates. The non linear deflection is finally
203 converted into linear displacement by a mechanical coupler to produce a sensor with a linear
204 output characteristic. The sensitivity of the PDMS-based touch mode capacitive pressure
205 for simulated and calculated data for a 20 [μm] diaphragm thickness is 0.03685 [fF/MPa] and
206 0.03467 [fF/MPa], respectively. The sensitivity of the PMMA-based touch mode capacitive
207 pressure is 0.03929 [fF/MPa] for simulated pressure and 0.03748 [fF/MPa] for calculated
208 pressure for a 20 [μm] thick diaphragm. The sensitivity of the PMMA based TMCPS is higher
209 than the PDMS based TMCPS.
210
211

222

223

REFERENCES

224

225

226

1. Chen D., Cai Y., Huang M. C. Customizable Pressure Sensor Array: Design and Evaluation. *IEEE Sensors Journal*. 2018;18(15):6337-6344.

227

228

229

2. Yang W., Yang Q., Yan R., Zhang W., Yan X., Gao F., Yan W. Dynamic Response of Pressure Sensor With Magnetic Liquids. *IEEE Transactions on Applied Superconductivity*. 2010;20(3):1860-1863.

230

231

232

3. Li L., Wang L., Qin L., Lv Y. The theoretical model of 1-3-2 piezocomposites. *IEEE Transactions on Ultrasonics, Ferroelectrics, and Frequency Control*, 2009;56(7):1476-1482.

233

234

4. Shu L., Tao X., Feng D. D. A New Approach for Readout of Resistive Sensor Arrays for Wearable Electronic Applications. *IEEE Sensors Journal*. 2015;15(1):442-452.

235

236

5. Bakhoun E. G., Cheng M. H. M. High-Sensitivity Inductive Pressure Sensor. *IEEE Transactions on Instrumentation and Measurement*. 2011;60(8):2960-2966.

237

238

239

6. Houri C. G., Talbi A., Viard R., Gallas Q., Garnier E., Molton P., Delva J., Merlen A., Pernod, P. Robust thermal microstructure for designing flow sensors and pressure sensors. In *Proceedings of the 2017 IEEE Sensors*. 2017:1-3.

240

241

242

7. Bera S. C., Mandal N., Sarkar R. Study of a Pressure Transmitter Using an Improved Inductance Bridge Network and Bourdon Tube as Transducer. *IEEE Transactions on Instrumentation and Measurement*. 2011;60(4):1453-1460.

243

244

245

8. Luo J., Zhang L, Wu T., Song H., Tang C. Flexible piezoelectric pressure sensor with high sensitivity for electronic skin using near-field electrohydrodynamic direct-writing method. *Extreme Mechanics Letters*. 2021;48:101279.

246

247

248

9. Houri C. G., Talbi A., Viard R., Gallas Q., Garnier E., Molton P., Delva J., Merlen A., Pernod P. MEMS high temperature gradient sensor for skin-friction measurements in highly turbulent flows. In *Proceedings of the 2019 IEEE Sensors*. 2019: 9749 – 9755.

249

250

251

252

10. Alveringh D., Schut T. V. P., Wiegerink R. J., Sparreboom W., Lötters J. C. Resistive pressure sensors integrated with a coriolis mass flow sensor. In *Proceedings of the 19th International Conference on Solid-State Sensors, Actuators and Microsystems (TRANSDUCERS)*.2017:1167-1170.

- 253 11. Meetei M. S., Singh H. S., Singh A. D., Majumder S. A novel design and optimization for
254 beam bridge piezoelectric pressure sensor. 2020;11(12):2687-2701.
- 255 12. Meetei M. S., Singh H. S. Modelling and Simulation of a Diaphragm based Touch Mode
256 Capacitive Pressure Sensor (DTMCPS). International Journal of Mechanical
257 Engineering. 2021;6(3):2784-2788.
- 258 13. Cotton D. P. J., Graz I. M., Lacour S. P. A Multifunctional Capacitive Sensor for
259 Stretchable Electronic Skins. IEEE Sensors Journal. 2009;9(12):2008-2009.
- 260 14. Timoshenko S. P., Woinowsky-Krieger, S. Theory of Plates and Shells. Mc Graw Hill;
261 New York:1959.
- 262 15. Ugural A. C. Plates and shells: theory and analysis. Boca Raton: London New York;
263 2018.
- 264 16. Bao M. Analysis and Design Principles of MEMS Devices. Elsevier Science: Amsterdam
265 Netherlands;2005.